nanomaterials

MDPI

A self-assembly of single layer of Co nanorods to reveal the magnetostatic interaction mechanism

Hongyu Du#, Min Zhang#, ke Yang, Baohe Li* and Zhenhui Ma*

Department of Physics, Beijing Technology and Business University, Beijing, 100048, China.
The Hongyu Du and Min Zhang contribute this work equally.
* Correspondence: Author: Baohe Li, lbhe@th.btbu.edu.cn; Zhenhui Ma, mazh@btbu.edu.cn

Abstract: In this work, we report a self-assembly method to fabricate single layer of Co nanorods to study their magnetostatic interaction behavior. The Co nanorods with cambered and flat tips are synthesized using a solvothermal route and an alcohol-thermal method, respectively. Both of them represent hard magnetic features. Co nanorods with cambered tips have an average diameter of 10 nm and length of 100 nm with coercivity of 6.4 kOe, and flat-tip nanorods with a 30 nm diameter and 100 nm length exhibit a coercivity of 4.9 kOe. They are further assembled on the surface of water in assistance of surfactants. The results demonstrate that the assembly type is dependent on the magnetic induction lines direction. For Co nanorods with flat tips, most of magnetic induction lines are parallel to the length direction, leading to an assembly tip to tip. For Co nanorods with cambered tips, they are prone to holding together side by side for their random magnetic induction lines. Under an applied field, the Co nanorods with flat tips can be further aligned into single layer of Co nanorods. Our work gives a possible mechanism for magnetic interaction of Co nanorods and provides a method to study their magnetic behavior.

Keywords: Nanomagnets; Co nanorods; Solvothermal route; Alcohol-thermal method; Magnetic interaction.

1. Introduction

Nanomagnets, with strong magnetic properties and small volume, have been considered as the key materials to magnetic and electronic devices, which exhibits important applications in artificial intelligence, intelligent robot, wind turbine and electromobile [1-12]. Compared with rare earth based nanomagnets, the rare earth free nanomagnets earn more attentions for their high chemical stability and low cost [13-16]. However, these rare earth free nanomagnets present small coercivity due to their relatively low magnetocrystalline anisotropy. One strategy to fabricate one-dimensional nanowires or nanorods by the special methods can resolve above problem, since the direction along nanorods length has the lowest demagnetizing field [17-19]. As a result, the shape anisotropy can be summed to magnetocrystalline anisotropy, leading to these nanorods with a larger coercivity than spherical particles. When an external field was applied in these particles, they can orient along the external field direction. Therefore, the system of magnetic nanorods along applied field will exhibit an enhanced coercivity, high remanence (M_r) and large energy product.

Hexagonal structured Co has a magnetocrystalline anisotropy constant (K_1 = 440 kJ/m^3), and its bulk has a high saturation magnetization (M_s = 160 emu/g) [20]. Therefore, in the last few decades, Co was always considered as a soft magnetic material since its magnetocrystalline anisotropy is far smaller than those of some well-known hard magnetic structures, such as samarium−cobalt ($SmCo_5$) (17200 kJ/m^3) and neodymium iron boron ($Nd_2Fe_{14}B$) (4900 kJ/m^3) [21-24]. Recently, the Co nanowires have been a potential candidate to rare earth free nanomagnet because the Co nanowires with their length direction along [002] (the easy magnetization axis direction) can obtain a large coercivity. To obtain such shape-anisotropic Co nanowires, a conventional approach via electrochemical deposition of Co into a porous alumina template was employed, which yielded an enhanced coercivity from an aligned Co nanowire array but it is lower than the theoretical value because of the polycrystalline structure [25]. Recently, a solution-phase synthesis has been used to reduce a cobalt salt using an organic polyalcohol. The resulted Co nanowires possessed a single crystal structure and their lengths (50-300 nm) and diameters (5-30 nm) can be tuned to achieve high performance [26-29]. As a consequence, the aligned Co nanomagnet fabricated by nanowires exhibits an ultrahigh coercivity up to 10 kOe, which exceeded the theoretical value of bulk Co material (7.6 kOe) [27]. The high coercivity originated from a sum of magnetocrystalline anisotropy field (7.6 kOe) and shape anisotropy field (9 kOe) [27].

It is worth noting that the magnetic alignment is a key parameter to obtain large coercivity and high M_r. To obtain an aligned nanomagnet, these as-prepared Co nanowires or nanorods have to be mixed with epoxy and aligned under an applied field [26-27]. In such nanomagnet, the aligned Co nanowires were stacked layers by layers, and the magnetostatic interaction among Co layers will have an obvious influence on alignment and magnetic performance. However, the single layer of aligned Co nanorods was very hard to prepare using current methods, which was valuable to study the magnetostatic interaction of nanomagnets.

Here, we develop a novel method to obtain single layer of aligned Co nanorods. First, we synthesized different shaped Co nanorods by solvothermal route (the nanorods with flat tips) and alcohol-thermal method (the nanorods with cambered tips), respectively. These nanorods were further aligned using a self-assembly strategy. As a result, a well-aligned single layer of nanorods was obtained under an applied field. Their self-assembly behaviors are further studied without an applied field. It is found that the nanorods with flat tips are prone to aligning tip to tip and the nanorods with cambered tips are easy to hold together side by side. Furthermore, we analyzed the magnetic interaction mechanism of Co nanorods with different tips to demonstrate their assembly behaviors. Our work provides an important reference to study magnetostatic interaction of shape anisotropic nanomagnets.

2. Experiments and Methods

2.1 Chemicals and Materials:

All chemicals were used without further purifications. Cobalt chloride hexahydrate ($CoCl_2 \cdot 6H_2O$, 98%, M_w=237.93), sodium laurate ($C_{11}H_{23}COONa$, ≥99%, M_w= 222.30), oleylamine (OAm, 70%, M_w= 267.49), oleic acid (OA, 90%, M_w= 282.46), 2-butanediol (BEG, 98%, M_w= 90.12), Ruthenium chloride (III) hydrate ($RuCl_3 \cdot xH_2O$, 99.98%, M_w= 207.43), hexadecylamine (HDA, 98%, M_w= 241.46), hexane (≥99%, M_w= 86.18), methylbenzene (=99.8%, M_w= 82.14) and chloroform (≥99.8%, M_w= 119.38) were purchased from Sigma-Aldrich.

2.2. The synthesis of cobalt (II) laurate

The Cobalt (II) laurate ($Co(C_{11}H_{23}COO)_2$) was prepared by mixing $C_{11}H_{23}COONa$ and $CoCl_2$. In a typical reaction, 9.3366 g of $C_{11}H_{23}COONa$ were dissolved in 30 mL of deionized water with a mechanical stirrer in three-neck flask, which was heated to 60 °C using water bath. Then, 5.000 g $CoCl_2$ were dissolved in 10 mL deionized water in another flask, forming $CoCl_2$ aqueous solution. The latter was added into former system dropwise with vigorous stirring. The mixture was stirred for a further 30 min and kept at 60 °C to obtain a purple precipitate, which was centrifuged at 8000 rpm for 8 min, and washed three times with 50 mL deionized water and methanol, respectively. The as-prepared precipitate was further dried in an air oven at 60 °C.

2.3. The synthesis of cobalt nanorods using a solvothermal route

The Co nanorods was first synthesized by reducing Co-laurate in BEG. In a typical synthesis, 2.0700 g of Co-laurate, 0.5810 g of HDA, and 0.0037 g of $RuCl_3$ were dissolved in 60 mL of BEG in three-neck flask, which was heated to 90 °C for 30 min to obtain a uniform solution. Then, the solution was transferred into a teflon enclosure (100 mL), and was further heated to 250 °C for 60 min with a heating rate of 15 °C/min for a solvothermal route. After cooling to room temperature, the black magnetic product was precipitated and washed by toluene by centrifuging at 6000 rpm for 5 min at least 3 times.

2.4. The synthesis of cobalt nanorods using an alcohol-thermal method

In a representative synthesis, 0.6113 g of Co-laurate, 0.0077 g of $RuCl_3$, and 0.4640 g of NaOH were added to 15.5 mL of BEG. Under mechanical stirring, the reaction mixture was heated to 100 °C for 30 min to obtain the uniform solution. And then, the solution was further heated to 175 °C with a temperature ramping rate of 7 °C/min, and was maintained at this temperature for 30 min. After cooling to room temperature, the black powder was recovered by centrifugation at 6000 rpm for 5 min, washed with ethanol for 3 times. For short Co nanorods, the mechanical stirring rate was 100 r/min; and for the long Co nanorods, the rate was set to 50 r/min.

2.5. The self-assembly of Co nanorods

To obtain single-layer Co nanorods assemble, we use OA and OAm with volume ratio of 1:3 as the surfactants. First, 0.0010 g of Co nanorods were dispersed 20 ml of above mixed solution to achieve the ligand exchange under ultrasonic shock for 24 h. Then, these nanorods were recovered by centrifugation and washed using hexane for 3 times. And then, the centrifuged Co nanorods were dispersed again in 20 ml methylbenzene using ultrasonic shock. 1-2 droplets of Co nanorods/methylbenzene were dropped on the smooth surface of water, and the system was sealed using glass sheets to make the methylbenzene evaporate slowly for 4h. A TEM grid was used to collect the self-assembly samples. For the magnetic field assisted self-assembly, a magnet was closed the water surface during the evaporation of organic solution. The other surfactant like HDA and PVP, and other solution like hexane and chloroform were employed to replace the OA/OAm and methylbenzene, respectively. But they failed to get the well-aligned Co layers.

2.6. Characterization

The Co nanorods structure was studied by X-ray diffraction (XRD, D/MAX 2200 PC) with Cu-K_α radiation (λ=0.15418 nm). The microstructure and morphology of the samples were analyzed by transmission electron microscopy (TEM, Philips CM 20). HRTEM were performed on JEM-2100F. The magnetic properties were measured at room temperature using a vibrating sample magnetometer (VSM) under a maximum applied field of 30 kOe. And all of magnetic properties were measured using the random aligned Co rods.

3. Results and discussions

3.1. The self-assembly of Co nanorods with cambered tips

We first synthesized Co nanorods with cambered tips by solvothermal route using a hydrothermal reactor as shown in **Figure 1**. The XRD pattern (**Figure 1A**) demonstrates that the solvothermal route yields hexagonal structure Co particles. All broad peaks have a good match with standard Co (JCPDS No. 01-1278) pattern. There are obvious differences among the width of diffraction peaks (100), (002) and (101). The broader (002) plane indicates the smaller size perpendicular to [002] than other directions, suggesting the shape anisotropic particles are obtained. The TEM results further confirm the successful synthesis of shape anisotropic Co nanoparticles. It can be seen from **Figure 1B-C** that the solvothermal reaction generates the uniform Co nanorods with their diameter about 10 nm and length 100-150 nm. These as-prepared Co nanorods have obvious cambered tips, and are prone to distribution side by side. The microstructure of the Co nanorod was further observed using HRTEM, as shown in **Figure 1D**. Along the length direction, the interplanar spacing of 0.20 nm were observed, matching well with hcp-Co (002) plane, which indicates that the length direction is consistent with [002] direction. As we known, the [002] direction is the easy magnetization axis (c-axis). Therefore, such shape can contribute a large shape anisotropy, which can combine with magnetocrystalline anisotropy and give a high coercivity.

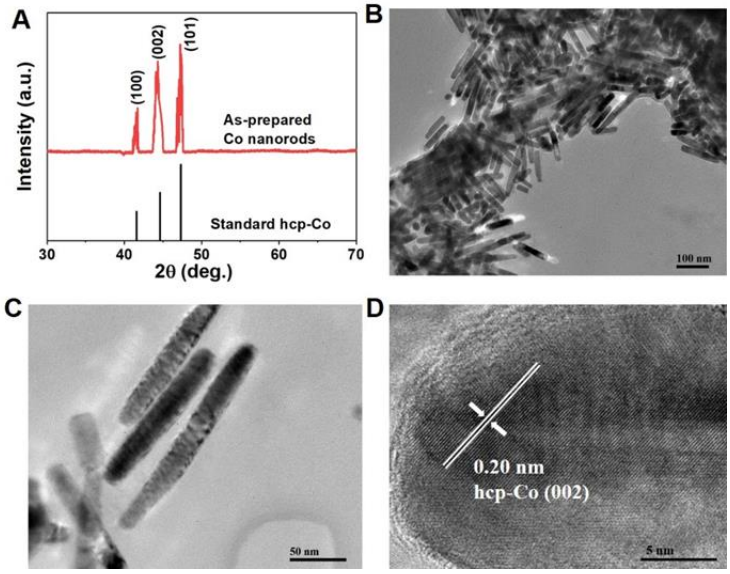


Figure 1. The Co nanorods with cambered tips by solvothermal route: (A) XRD pattern compared with standard hcp-Co (JCPDS No. 01-1278); (B) and (C) TEM images with different magnification; (D) HRTEM image.

We try to make these Co nanorods self-assembly by the molecular force of surfactant without any magnetic field. The OA and OAm were employed as the surfactant, and the results are shown in **Figure 2**. From the TEM images in **Figure 2A-C**, the Co nanorods were well aligned into an assembly. Unfortunately, these Co nanorods are not aligned

along a particular direction. These self-assembly presents radial, and the direction is from the center to all round. This phenomenon can be explained that some aggregates of Co nanorods become a hard magnetic core like a spherical magnet, which yields a strong radial magnetic field, making other nanorods align along the magnetic field (**Figure 2B**). We can further observe that these nanorods are aligned side by side (**Figure 2C**), which may be caused by the magnetostatic interactions among nanorods. We also try to use other surfactants to do the self-assembly, but they failed to obtain well alignment due to the strong magnetic interaction. This result demonstrates that the magnetic interactions among nanorods are far stronger than molecular interactions of surfactants. We measured the magnetic hysteresis loop of random Co nanorods at room temperature (**Figure 2D**), which exhibits a large coercivity of 6.4 kOe and high M_s of 148.3 emu/g under 2.5 kOe field. Once these nanorods were aligned into nanomagnet using a magnetic field, their coercivity will exceed 10 kOe, being an excellent candidate for strong magnetic materials [30].

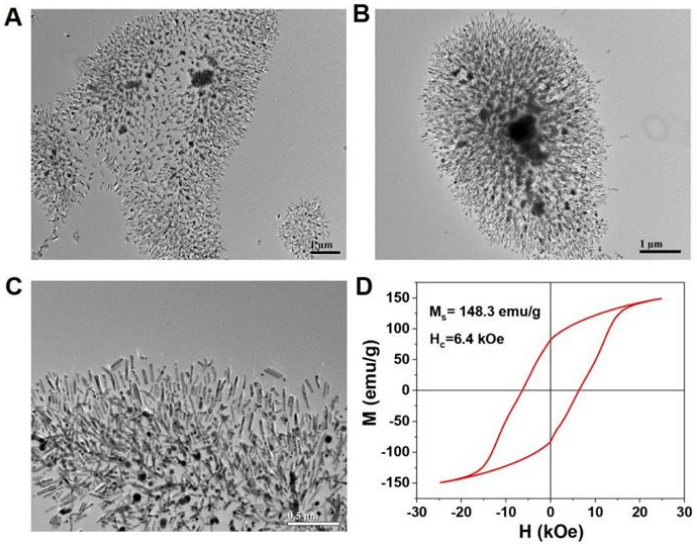


Figure 2. (A-C) The TEM images of self-assembly Co nanorods with cambered tips by solvothermal route; (D) Magnetic hysteresis loop of Co nanorods at room temperature.

3.2. The self-assembly of Co nanorods with flat tips

As a comparison, we also synthesized Co nanorods with flat tips by alcohol-thermal method using a reflux set, as shown in **Figure 3**. The XRD pattern (**Figure 3A**, the samples were prepared with a stirring rate of 100 r/min) can correspond to hexagonal structure Co very well. And we also can find the different peaks width for (100), (002) and (101) plane, which indicates the as-prepared Co particles have a shape anisotropy. Different from Co nanorods obtained from solvothermal method, the diffraction peaks of Co (002) planes exhibit an obvious enhancement by comparing with the standard peaks. This may suggest that these Co nanorods have a self-orientation effect. The **Figure 3B-C** give the TEM images of Co nanorods. The uniform Co nanorods display bamboo-like shape with an average diameter of ~30 nm and length of ~100 nm. It is interesting that these Co nanorods have larger tips than their body and their tips exhibit a flat plane. Without any magnetic field or surfactant, several Co nanorods are self-oriented tip to tip, forming a bamboo-like shape, totally different from these Co nanorods with cambered tips. We further synthesized a kind of longer Co nanorods by using a lower stirring rate of 50 r/min, as shown in **Figure 3D**. With the decrease of stirring rate, there is no obvious change for the diameter of as-prepared Co nanorods, but their length does increase to 200 nm from 100 nm. Certainly, these longer Co nanorods still represent larger tips and smaller body, and they also have a self-orientation effect by going tip to tip. This demonstrates that the mechanical

stirring can interrupt the growth of nanorods from the length direction, which can be explained that the growth of long Co nanorods needs Co^{2+} continuously feeding. With the increase of stirring rate, homogenizing of solution can hinder local increment of Co^{2+} concentration in the solution [31-32]. As a result, the growth of Co nanorods from the length direction was interrupted, forming multiple shorter nanorods.

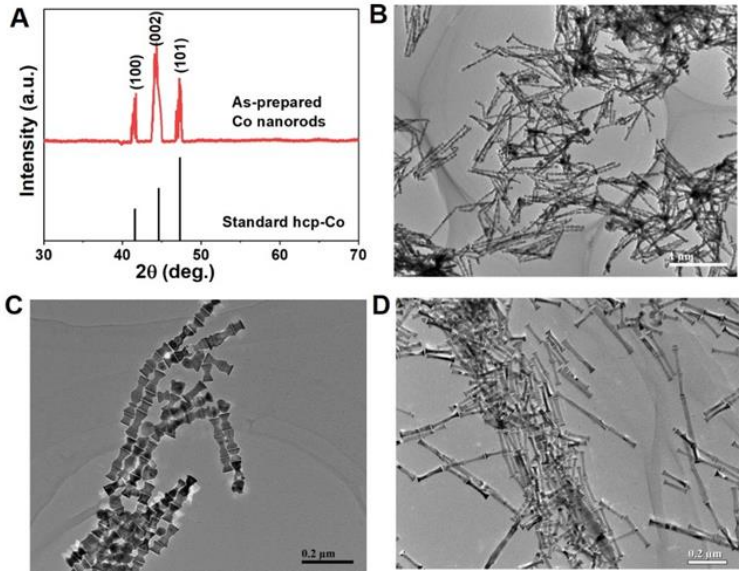


Figure 3. The Co nanorods with flat tips by alcohol-thermal method. (A) XRD pattern compared with standard hcp-Co (JCPDS No. 01-1278); (B - C) TEM images of Co nanorods with 100 r/min stirring rate; (D) TEM image of Co nanorods with 50 r/min stirring rate.

The magnetic hysteresis loop of random Co nanorods with the length of 100 nm was measured at room temperature using VSM. As shown in **Figure 4**, these Co nanorods exhibit a coercivity of 4.9 kOe and M_s of 146.5 emu/g at an applied field of 2.5 kOe. Compared with Co nanorods with cambered tips, these Co nanorods with flat tips exhibit lower magnetic performance. This may be ascribed to two reasons. On the one hand, the ratio of length to diameter (L/D) is a key factor to the coercivity due to the shape anisotropy. In general, the higher ratio will lead to larger coercivity [33]. In our work, the Co nanorods with cambered tips have a L/D of ~10, while the L/D value for Co nanorods with flat tips is only ~4. On the other hand, the Co nanorods with flat tips have smaller coercivity than cambered tips even though they have the similar L/D. Because Co nanorods with flat tips have more defects (stacking fault) between the tips and bodies, which can lead to a high demagnetizing filed and causes the low coercivity [34].

The coercive mechanism of Co nanorods is totally different from small-sized Co nanoparticles or clusters. As we known, the magnetic particles have the largest coercivity at the key size from multiple-domain to single-domain structure, and the key size is about 30 nm for Co particles [17]. Thus, our Co nanorods with a diameter about 10 nm and length 100-150 nm display a relatively higher coercivity than small-sized Co particles (several nanometers). Furthermore, these Co nanorods have been confirmed to be single-domain structure in previous work [27]. And for Co clusters with small size, they are superparamagnetic and thus have no coercivity at room temperature since their magnetocrystalline anisotropy at this size cannot compete with thermal disturbance [35]. More importantly, the coercivity of hcp-Co nanorods is mainly originated from shape anisotropy rather than magnetocrystalline anisotropy. In other words, the high L/D lead to their large coercivity, which can be confirmed by many reports [33].

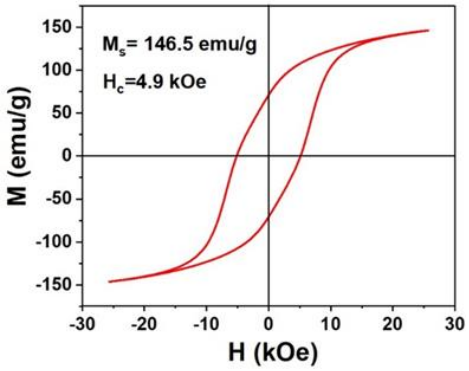


Figure 4. Magnetic hysteresis loop of Co nanorods with flat tips at room temperature.

These as-prepared Co nanorods with flat tips were further assembled on the water solution surface by using OA and OAm as the surfactant. Without any external field, driven by the molecular force of surfactant and magnetostatic force, these Co nanorods tend to align tip to tip and form long nanochains, but there is obvious space between aligned nanochains (**Figure 5A**). Although this alignment cannot reach our expectation, most of as-formed Co nanochains do present consistent direction, which has an obvious improvement than the Co nanorods with cambered tips. We also can observe the well-aligned Co nanorods in some view of TEM, as shown in **Figure 5B**. In these regions, these nanorods first form straight nanochains, and then these nanochains assemble into single layer. Unfortunately, these regions are isolated each other, hard to form high quality single-layer self-assembly. This result may be caused by magnetostatic interaction, which be discussed in next section in detail. To obtain high quality Co nanorods assemble, an external field was applied during self-assembly process. The results are shown in **Figure 5C-D**. According to XRD pattern in **Figure 5C**, the assembled Co nanorods under external field only display a single diffraction peak around 44.5°, which can be indexed to hcp-Co (002) plane. As we known, the easy axis of Co nanorods is [002] direction, which is also the length direction. When these nanorods were aligned, all of Co nanorods display the same direction. As a result, the X-ray only detected the (002) plane. The TEM image in **Figure 5D** demonstrates that these Co nanorods with ~100 nm length were well aligned into single layer along the magnetic field direction, further confirming the XRD result. We further aligned Co nanorods with ~200 nm length under same conditions, but it failed to obtain good alignment, which can be explained that the stronger properties of Co nanorods are unfavorable to align due to the strong interaction with each other.

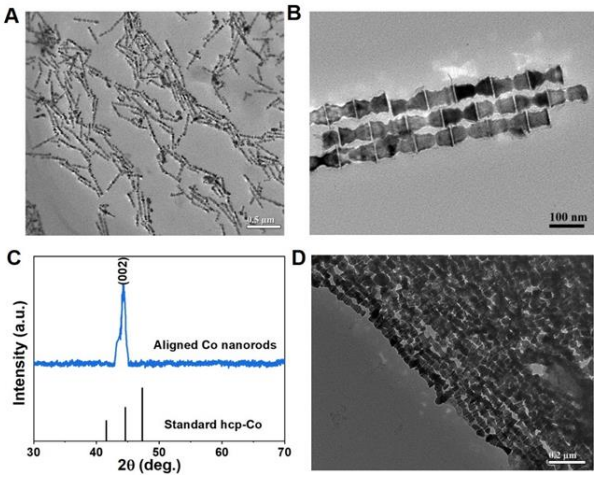


Figure 5. (A-B) The TEM images of self-assembly Co nanorods with flat tips without applied field; (C) XRD pattern of aligned Co nanorods under magnetic field compared with standard hcp-Co (JCPDS No. 01-1278); (D) TEM image of aligned Co nanorods under magnetic field.

3.3. The discussion of magnetostatic interaction mechanism

During self-assembly process, there is a competition between molecular interaction force and magnetostatic force. The former drives these nanorods align well, while the latter makes them random to reduce the magnetostatic energy. In our work, the magnetostatic force is obviously stronger than molecular interaction force. Therefore, we should analyze their behavior from the view of magnetostatic interaction.

We analyze the magnetostatic interaction mechanism using magnetic induction line distribution, as shown in **Figure 6**. For all of Co nanorods they can be regarded as a tiny magnet at nanoscale, and the two tips of nanorods correspond to their N-S poles (**Figure 6A1** and **6B1**) [36]. And the magnetic induction lines at two tips should be perpendicular to their tips.

For the Co nanorods with flat tips, they have larger tips. Therefore, most of magnetic induction lines are perpendicular to the flat tips and thus parallel to [002] direction (**Figure 6A1**). As a result, these Co nanorods are prone to holding together tip to tip since the magnetic induction lines direction for N pole of one Co nanorod is consistent with the S pole of another Co nanorod (**Figure 6A2**). If these nanochains assembled by Co nanorods have same direction for N-S poles, they would present mutual exclusion and thus these nanochains would be separated from each other (**Figure 6A3**). If they have the opposite N-S poles, they would hold together again by connecting the third nanochains and rotate at a certain angle to keep the minimum energy (**Figure 6A4-A5**). When an external field was applied, these nanochains can rotate into the magnetic field direction to achieve alignment.

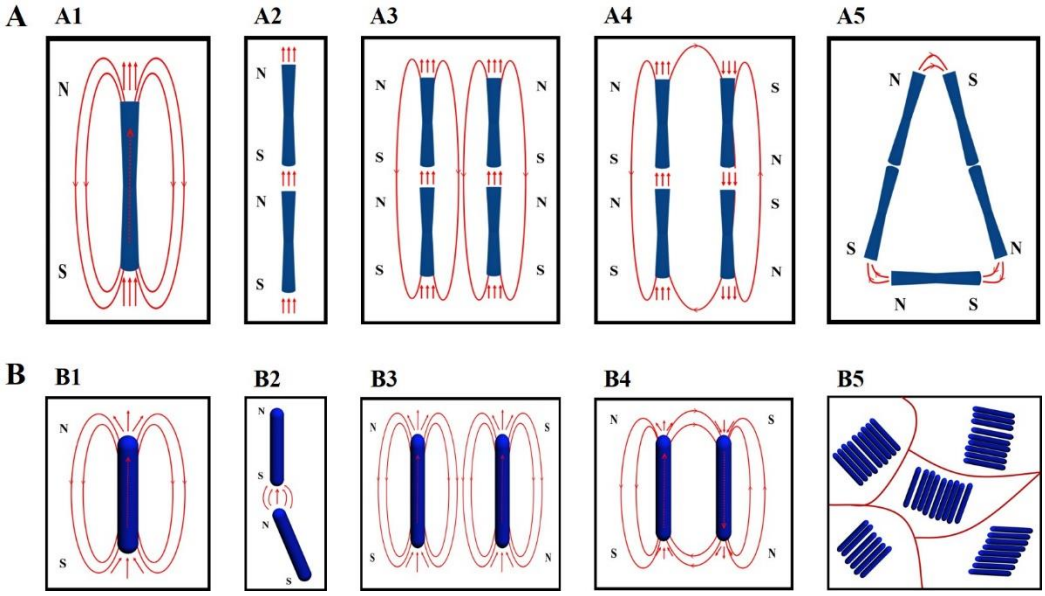


Figure 6. The scheme of magnetostatic interaction mechanism. (A) Co nanorods with flat tips; (B) Co nanorods with cambered tips.

For the Co nanorods with cambered tips, they have smaller tips. Due to the special morphology, they only have very few magnetic induction lines parallel to c-axis. Most of magnetic inductions line are random (**Figure 6B1**). Therefore, tip to tip assemble is very unstable. It needs to rotate at a certain angle to reduce the energy of system (**Figure 6B2**). On this occasion, these nanorods are prone to holding together side by side for their ran-

dom magnetic induction lines, since there are some angles between most of magnetic induction lines and nanorods c-axis (**Figure 6B3-B4**). Despite of that, the alignment side by side was only confined into several nanorods [37]. These clusters assembled by several nanorods with the same direction can be regarded as a "magnetic domain" and the system is like a "multidomain magnet" (**Figure 6B5**). To keep the minimum energy of the whole system, these "magnetic domain" directions are distributed randomly. When an external field or self-generated field (some nanorods aggregate like a magnet in **Figure 2B**) was applied, these "magnetic domains" can rotate into the magnetic field direction to achieve alignment.

4. Conclusions

In summary, we synthesized two kinds of Co nanorods, one with cambered tips and another with flat tips, and achieve a self-assembly of single layer of Co nanorods to study their magnetostatic interaction behavior. The as-synthesized Co nanorods with cambered tips have an average diameter of 10 nm and length of 100 nm with coercivity of 6.4 kOe, and flat-tip nanorods with a 30 nm diameter and 100 nm length exhibit a coercivity of 4.9 kOe. These Co nanorods were first assembled on the surface of water without magnetic field. It is found that the Co nanorods with cambered tips are prone to aligning side by side, while the Co nanorods with flat tips are easy to hold together tip to tip due to the magnetostatic interaction. Under an applied field, the Co nanorods with flat tips can be further aligned into single layer of Co nanorods. Furthermore, we study the magnetostatic interaction mechanism using magnetic induction lines. Because each nanorod can be considered as a magnet, the flay tips of Co nanorods are like N and S poles of magnet. Therefore, they are easy to hold together tip to tip since most of magnetic induction lines are parallel to the length direction. For Co nanorods with cambered tips, they are prone to holding together side by side to form clusters for their random magnetic induction lines. Our work provides a method to study magnetic interaction of shape anisotropy.

Acknowledgments: This work was financially supported by the Capacity Building for Scientific and Technological Innovation Services Project of Beijing Technology and Business University (No. 19008021178), and Beijing Technology and Business University Research Team Construction Project (No. 19008022165).

Conflicts of Interest: The authors declare no conflict of interest.

References

1. Ma, Z. H.; Yue, M.; Liu, H.; Yin, Z. Y.; Wei, K. C.; Guan, H. Q.; Lin, H. H.; Shen, M. Q.; An, S. Z.; Wu, Q.; Sun, S. H., Stabilizing hard magnetic $SmCo_5$ nanoparticles by n-doped graphitic carbon layer. *Journal of the American Chemical Society* **2020,** *142* (18), 8440-8446.
2. Wang, S.; Xu, J.; Li, W.; Sun, S.; Gao, S.; Hou, Y., Magnetic nanostructures: Rational design and fabrication strategies toward diverse applications. *Chemical Reviews* **2022,** *122* (6), 5411-5475.
3. Zhao, P.; Luo, Y.; Yu, D. B.; Peng, H. J.; Yan, W. L.; Wang, Z. L.; Bai, X. Y., Preparation and properties of hot-deformed magnets processed from nanocrystalline/amorphous Nd-Fe-B powders. *Rare Metals* **2021,** *40* (8), 2033-2039.
4. Ma, Z.; Tian, H.; Cong, L.; Wu, Q.; Yue, M.; Sun, S., A flame-reaction method for the large-scale synthesis of high-performance Sm_xCo_y nanomagnets. *Angewandte Chemie-International Edition* **2019,** *58* (41), 14509-14512.
5. Yang, W.; Liang, D.; Kong, X.; Yang, J., Neutron diffraction studies of permanent magnetic materials. *Rare Metals* **2020,** *39* (1), 13-21.
6. Shen, B.; Yu, C.; Baker, A. A.; McCall, S. K.; Yu, Y.; Su, D.; Yin, Z.; Liu, H.; Li, J.; Sun, S., Chemical synthesis of magnetically hard and strong rare earth metal based nanomagnets. *Angewandte Chemie-International Edition* **2019,** *58* (2), 602-606.
7. Ma, Z.; Du, H., Stabilizing interface of $SmCo_5$/Co nanocomposites by graphene shells. *Rare Metals* **2022,** *41* (4), 1223-1229.
8. Xu, G.; Lu, H.; Guo, K.; Tang, F.; Song, X., Predictions on the phase constitution of $SmCo_{7-X}M_x$ alloys by data mining. *Nanomaterials* **2022,** *12* (9), 1452.
9. Guan, H. Q.; Huang, S. S.; Ding, J. H.; Tian, F. Y.; Xu, Q.; Zhao, J. J., Chemical environment and magnetic moment effects on point defect formations in CoCrNi-based concentrated solid-solution alloys. *Acta Materialia* **2020,** *187*, 122-134.

10. Zhang, G.; Zhang, Z.; Sun, M.; Yu, Y.; Wang, J.; Cai, S. B., The influence of the temperature on the dynamic behaviors of magnetorheological gel. *Advanced Engineering Materials.* **2020,** 2101680.
11. Lu, C. J.; Zhou, H.; Li, L. F.; Yang, A. C.; Xu, C. B.; Ou, Z. Y.; Wang, J. Q.; Wang, X.; Tian, F., Split-core magnetoelectric current sensor and wireless current measurement application. *Measurement* **2022,** *188*, 110527.
12. Li, S. M.; Zhang, S. Q.; Zhao, R. Q., Regulating the electronic and magnetic properties of 1T'-ReS_2 by fabricating nanoribbons and transition-metal doping: a theoretical study. *Nanoscale* **2022,** *14* (23), 8454-8462.
13. Cui, J.; Kramer, M.; Zhou, L.; Liu, F.; Gabay, A.; Hadjipanayis, G.; Balasubramanian, B.; Sellmyer, D., Current progress and future challenges in rare-earth-free permanent magnets. *Acta Materialia* **2018,** *158*, 118-137.
14. Li, H.; Wu, Q.; Yue, M.; Peng, Y.; Li, Y.; Liang, J.; Wang, D.; Zhang, J., Magnetization reversal in cobalt nanowires with combined magneto-crystalline and shape anisotropies. *Journal of Magnetism and Magnetic Materials* **2019,** *481*, 104-110.
15. Jia, Y.; Wu, Y.; Zhao, S.; Zuo, S.; Skokov, K. P.; Gutfleisch, O.; Jiang, C.; Xu, H., L1(0) rare-earth-free permanent magnets: The effects of twinning versus dislocations in Mn-Al magnets. *Physical Review Materials* **2020,** *4* (9), 094402.
16. Crisan, A. D.; Leca, A.; Bartha, C.; Dan, I.; Crisan, O., Magnetism and epsilon-tau phase transformation in MnAl-based nanocomposite magnets. *Nanomaterials* **2021,** *11* (4), 896.
17. Ma, Z.; Mohapatra, J.; Wei, K.; Liu, J. P.; Sun, S., Magnetic nanoparticles: Synthesis, anisotropy, and applications. *Chemical Reviews* **2021,** 10.1021/acs.chemrev.1c00860.
18. Proenca, M. P., Multifunctional magnetic nanowires and nanotubes. *Nanomaterials* **2022,** *12* (8), 1308.
19. Ma, Z.; Yue, M.; Wu, Q.; Li, C.; Yu, Y., Designing shape anisotropic $SmCo_5$ particles by chemical synthesis to reveal the morphological evolution mechanism. *Nanoscale* **2018,** *10* (22), 10377-10382.
20. Mohapatra, J.; Xing, M.; Elkins, J.; Liu, J. P., Hard and semi-hard magnetic materials based on cobalt and cobalt alloys. *Journal of Alloys and Compounds* **2020,** *824,* 153874.
21. Ma, Z.; Liang, J.; Ma, W.; Cong, L.; Wu, Q.; Yue, M., Chemically synthesized anisotropic $SmCo_5$ nanomagnets with a large energy product. *Nanoscale* **2019,** *11* (26), 12484-12488.
22. Ma, Z.; Zhang, T.; Jiang, C., A facile synthesis of high performance $SmCo_5$ nanoparticles. *Chemical Engineering Journal* **2015,** *264*, 610-616.
23. Zhang, D.; Zhu, R.; Yue, M.; Liu, W., Microstructure and magnetic properties of $SmCo_5$ sintered magnets. *Rare Metals* **2020,** *39* (11), 1295-1299.
24. Kwon, J.; Lee, D.; Yoo, D.; Park, S.; Cha, H.; Kwon, H.; Lee, J.; Lee, D., Enhancement of magnetic properties of hot pressed/die-upset Dy-free Nd-Fe-B magnets with Cu/Nd coating by wet process. *Rare Metals* **2020,** *39* (1), 48-54.
25. Zeng, H.; Zheng, M.; Skomski, R.; Sellmyer, D. J.; Liu, Y.; Menon, L.; Bandyopadhyay, S., Magnetic properties of self-assembled Co nanowires of varying length and diameter. *Journal of Applied Physics* **2000,** *87* (9), 4718-4720.
26. Gandha, K.; Mohapatra, J.; Liu, J. P., Coherent magnetization reversal and high magnetic coercivity in Co nanowire assemblies. *Journal of Magnetism and Magnetic Materials* **2017,** *438*, 41-45.
27. Gandha, K.; Elkins, K.; Poudyal, N.; Liu, X.; Liu, J. P., High energy product developed from cobalt nanowires. *Scientific Reports* **2014**, *4*(1), 1-5.
28. Anagnostopoulou, E.; Grindi, B.; Lacroix, L. M.; Ott, F.; Panagiotopoulos, I.; Viau, G., Dense arrays of cobalt nanorods as rare-earth free permanent magnets. *Nanoscale* **2016,** *8* (7), 4020-4029.
29. Ener, S.; Anagnostopoulou, E.; Dirba, I.; Lacroix, L.-M.; Ott, F.; Blon, T.; Piquemal, J.-Y.; Skokov, K. P.; Gutfleisch, O.; Viau, G., Consolidation of cobalt nanorods: A new route for rare-earth free nanostructured permanent magnets. *Acta Materialia* **2018,** *145*, 290-297.
30. Li, C.; Wu, Q.; Yue, M.; Xu, H.; Palaka, S.; Elkins, K.; Liu, J. P., Manipulation of morphology and magnetic properties in cobalt nanowires. *AIP Advances* **2017,** *7* (5), 056229.
31. Patil, S.; Kate, P. R.; Deshpande, J. B.; Kulkarni, A. A., Quantitative understanding of nucleation and growth kinetics of silver nanowires. *Chemical Engineering Journal* **2021**, *414*, 128711.
32. Amirjani, A.; Fatmehsari, D. H.; Marashi, P., Interactive effect of agitation rate and oxidative etching on growth mechanisms of silver nanowires during polyol process. *Journal of Experimental Nanoscience* **2015**, *10* (18), 1387-1400.
33. Li, H.; Wu, Q.; Peng, Y.; Xu, H.; Zhang, J.; Yue, M., Magnetic properties and magnetization reversal in Co nanowires with different morphology. *Journal of Magnetism and Magnetic Materials* **2019,** *469*, 203-210.
34. Mrad, K.; Schoenstein, F.; Nong, H. T. T.; Anagnostopoulou, E.; Viola, A.; Mouton, L.; Mercone, S.; Ricolleau, C.; Jouini, N.; Abderraba, M.; Lacroix, L. M.; Viau, G.; Piquemal, J. Y., Control of the crystal habit and magnetic properties of Co nanoparticles through the stirring rate. *Crystengcomm* **2017,** *19* (25), 3476-3484.
35. Jamet, M.; Wernsdorfer, W.; Thirion, C.; Mailly, D.; Dupuis, V.; Melinon, P.; Perez, A., Magnetic anisotropy of a single cobalt nanocluster. *Physical Review Letters* **2001,** *86* (20), 4676-4679.
36. Ma, Z.; Liu, H.; Yue, M., Magnetically recyclable Sm_2Co_{17}/Cu catalyst to chemoselectively reduce the 3-nitrostyrene into 3-vinylaniline under room temperature. *Nano Research* **2019,** *12* (12), 3085-3088.
37. Wu, Q.; Cong, L.; Yue, M.; Li, C.; Ma, Z.; Ma, X.; Wang, Y., A unique synthesis of rare-earth-Co-based single crystal particles by "self-aligned" Co nano-arrays. *Nanoscale* **2020,** *12* (26), 13958-13963.

400